

**SEISMIC WAVE GENERATION AND PROPAGATION FROM
COMPLEX 3D EXPLOSION SOURCES**

Jeffrey L. Stevens and Michael O'Brien

Science Applications International Corporation

Sponsored by the Air Force Research Laboratory

Contract No. FA9453-11-C-0232

Proposal No. BAA11-39

ABSTRACT

The objective of this new project is to investigate the generation of complex seismic waves by explosions in media with realistic three-dimensional (3D) heterogeneity, including topography. To do this, we use information on subsurface heterogeneity from nuclear test sites to develop 3D models that have the characteristics of the emplacement media for actual nuclear tests. We then run calculations in these structures and compare results with near-field, regional, and teleseismic data. Since we will never have complete information on the subsurface structure, we do not expect exact matches of the data, but if the heterogeneous characteristics of the media are correct, we expect the characteristics of the calculated data and the variations in the calculated data to be similar to those of the observed data. This is particularly true for the near-field data where additional complexities caused by the travel path are expected to be less pronounced. One of the objectives of this project is to address one of the most fundamental problems in nuclear monitoring seismology: why are shear waves generated by all underground nuclear explosions?

This project follows a recent project on 3D numerical modeling and wave propagation. In that project, we did the following: (1) developed a 3D nonlinear finite-element code designed for calculation of explosions in 3D heterogeneous media with well-tested material models and including gravity; (2) implemented interface codes, using the representation theorem, that propagate the numerical solution from the source region to regional and teleseismic distances; and (3) used the code to evaluate the effect of near-source heterogeneity, including nonlinear material property variations, elastic variability, and topography.

The reason that 3D calculations are important for understanding shear wave generation is that symmetry constraints imposed by one-dimensional (1D) and two-dimensional (2D) calculations act to suppress shear waves. To see this, consider trying to do an explosive experiment in which 2D axisymmetry is imposed. This requires that the motion generated by the explosion be identical in all horizontal directions through propagation of the shock wave, nonlinear deformation of the surrounding material, and rebound to a final state. Since the motion is never identical in all directions, shear waves will always be generated, and in fact shear waves are observed from all underground explosions.

One specific task of this project is to perform a 3D nonlinear calculation of the Nonproliferation Experiment (NPE). We have previously modeled this event with a 2D axisymmetric calculation and have rerun that calculation in 3D. We have also incorporated the actual topography of the site and run the calculation with 3D topography. The results show generation of an SH wave not present in the calculation without topography.

OBJECTIVES

The objective of this new project is to investigate the generation of complex seismic waves by explosions in media with realistic 3D heterogeneity, including topography. This is being accomplished using a recently completed 3D finite-element code designed for explosion calculations, together with a method based on the exact representation theorem for propagating complex 3D calculations to the local, regional, and teleseismic distances at which they are observed.

RESEARCH ACCOMPLISHED

Background and Motivation

This new project follows a previous project on 3D numerical modeling and wave propagation. In that project, we did the following:

1. Developed a 3D nonlinear finite element code designed for calculation of explosions in 3D heterogeneous media with well-tested material models and including gravity
2. Implemented interface codes, using the representation theorem, that propagate the numerical solution from the source region to regional and teleseismic distances
3. Used the code to evaluate the effect of near-source heterogeneity, including nonlinear material property variations, elastic variability, and topography

The reason that 3D calculations are important for understanding shear wave generation is that symmetry constraints imposed by 1D and 2D calculations act to suppress shear waves. To see this, consider trying to do an explosive experiment in which 2D axisymmetry is imposed. This requires that the motion generated by the explosion be identical in all horizontal directions through propagation of the shock wave, nonlinear deformation of the surrounding material, and rebound to a final state. Since the motion is never identical in all directions, shear waves will always be generated, and in fact shear waves are observed from all underground explosions. In this project we plan to develop realistic models for 3D near-source heterogeneity and then run 3D explosion calculations in these models. We are also performing calculations of specific events, starting with the NPE.

The CRAM3D Code

CRAM3D is an explicit 3D Lagrangian finite-element code designed to run on multiple processors (Stevens and Xu, 2010; Stevens et al, 2011). For an explosion simulation, the cavity is placed near the center of the grid and is enclosed by a spider grid, which facilitates applying the pressure boundary condition and rezoning elements (Figure 1). The well-tested nonlinear material models from CRAM2D have been implemented in CRAM3D. The code includes gravity and so includes the important effects that result from variation of overburden pressure with depth. The code also includes tensile cracking. Figure 2 shows a comparison of a 20-ton explosion calculation made with CRAM2D and CRAM3D. Figure 3 shows 3D cavity expansion from a 5-kt explosion and the surface motion from this calculation calculated with CRAM2D and CRAM3D. There is good agreement between CRAM2D and CRAM3D results on equivalent problems.

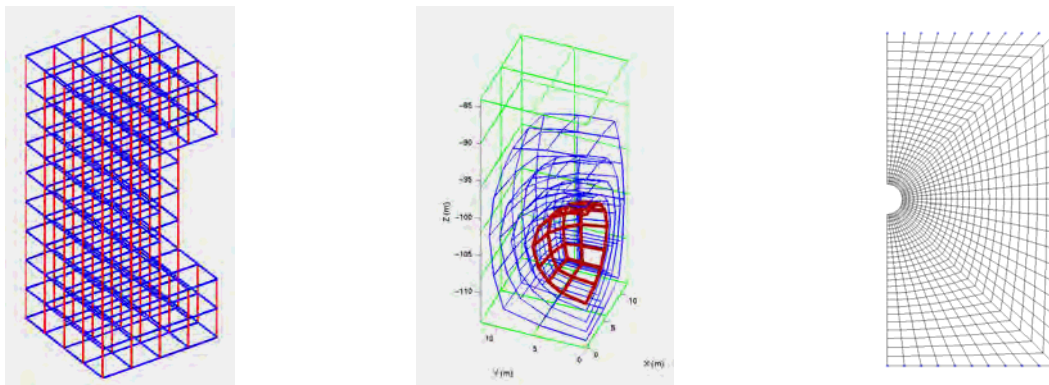


Figure 1. The CRAM3D finite -element outer grid (left) is rectangular. The inner grid (center) is shaped to match the shape of the explosion shock wave. CRAM2D uses a similar axisymmetric spider grid (right) in the region around the explosion.

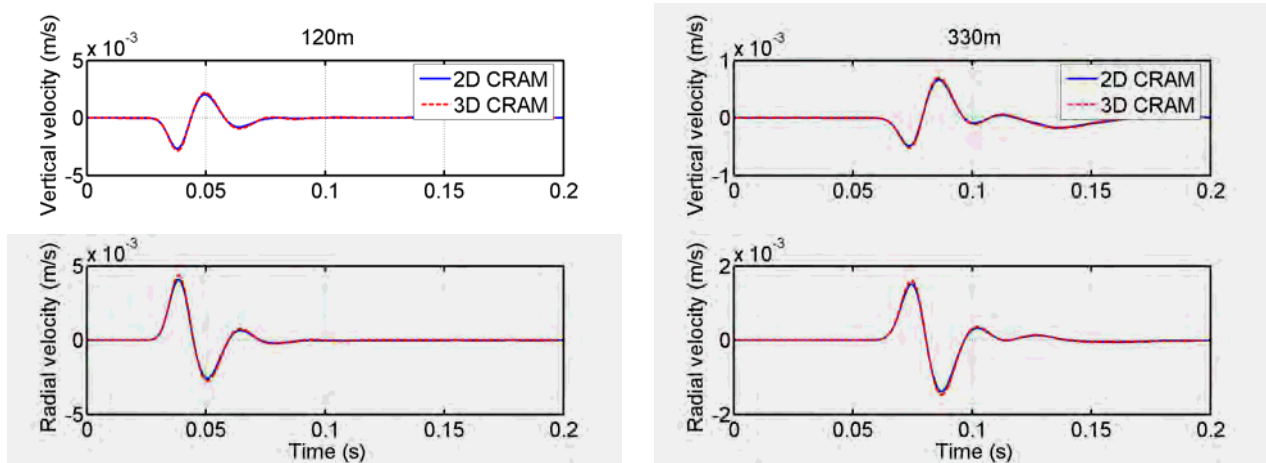


Figure 2. Dynamic response of a half-space nonlinear granite model (Stevens et al., 2003) to a 20-ton explosion in a 5-m spherical cavity buried at a depth of 102 m, using CRAM2D (blue) and CRAM3D (red). Comparisons of seismograms at two surface locations—120 m (left) and 330 m (right). The top row shows the vertical component; the bottom shows radial.

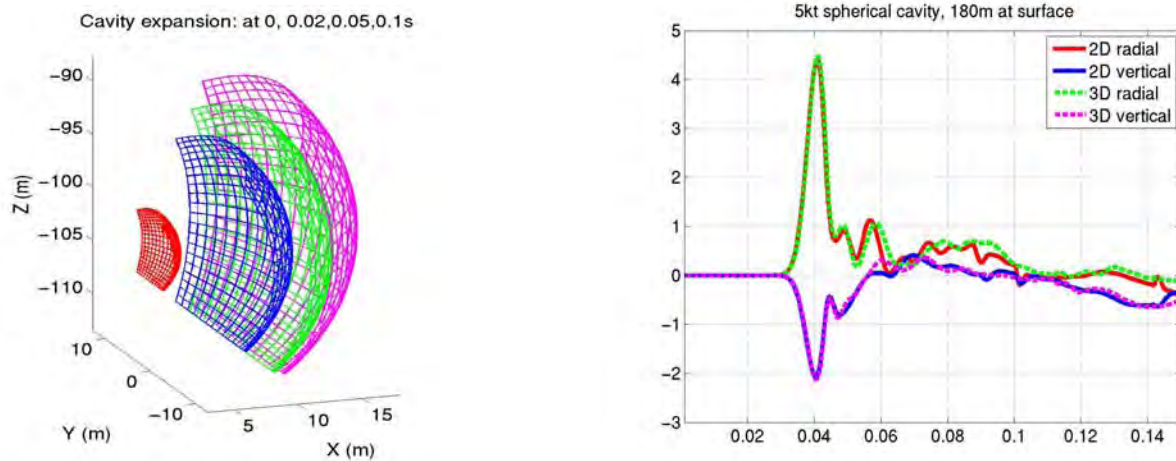


Figure 3. Cavity expansion for a 5-kt explosion in a 5-m spherical cavity (left) and a comparison of near-field motion at the surface from the 3D and equivalent 2D calculations.

Performance of CRAM3D

CRAM3D is designed to split the computational job among multiple processors. It does this by splitting the grid into logical/physical sections and uses the MPICH2 multiprocessor package to spawn multiple CRAM3D processes, each to perform computations on one of the grid sections. The inner grid is assigned to one process, while the outer grid is divided approximately evenly in the X direction and thus spread among the other processes. Using MPICH2 the processes may be spread among multiple processors, if available, or even multiple computers.

The goal is to reduce the run time of the computations so we track performance improvement by engaging more processors as the problem size changes. We have performed computations on a Dell R710 server with two 6-core Xeon X5680 (3.33 GHz) processors, thus making available 12 effectively independent processors. Figure 4 shows performance results that are typical of CRAM3D computations, illustrating the relationship observed between computation time and the number of processors employed for the computation, here for 100 cycles of CRAM3D on grids of the approximate dimensions $360 \times 240 \times 130$ (~3M zones). Computation time falls off more steeply than the expected $1/N$ (performance is better than expected) at low N ($\sim 1/N^{1.2}$). This occurs because there are fewer zones in

the inner grid, so that processor waits for the other processors to complete their work. As the number of processors is increased, this effect becomes smaller. Eventually we would expect the computation time to increase more slowly than $1/N$ because communication overhead between processors will become more important. Nevertheless, it is clear that the computation time decreases approximately linearly with the number of processors available, at least up to 12 processors. Performance was substantially better with the free gfortran compiler than with the commercial Portland Group (PG) Fortran compiler, apparently because PG Fortran intrinsically tries to use multiple processors, and there is no gain and likely some loss when processors are directed independently.

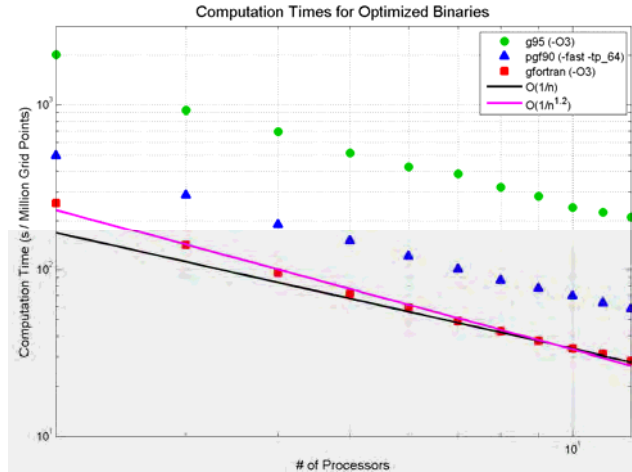


Figure 4. Computation time vs. the number of processors for a 100-cycle run of CRAM3D on grids with the approximate dimensions $360 \times 240 \times 130$.

Propagation with the Elastodynamic Representation Theorem

The representation theorem allows us to perform arbitrarily complex nonlinear calculations in the source region and then propagate them with an appropriate Green’s function. The representation theorem is exact. That is, no matter how complex the 3D motion is on the source region boundary, it will be correctly propagated by the representation theorem. The only exception is that it will not calculate the interaction of backscattered waves reflected from outside the source region with complexities of the source region. We use a plane-layered Green’s function outside the source region, although any Green’s function can be used.

In the 3D numerical finite-difference calculations, we save displacements and stresses due to the seismic source on a monitoring surface on the boundary of a rectangle (five planar surfaces, excluding the upper surface), and calculate Green’s functions from each point on the monitoring surface to the receiver, and so the synthetic seismogram at the receiver point X outside the monitoring surface is obtained by integrating over the monitoring surface S_M

$$u_i = \iint_{S_M} \left\{ G_j^i(\xi; X) * T_j^M(\xi) - u_j^M(\xi) * S_{jk}^i(\xi; X) n_k \right\} dA$$

in the frequency domain, where $G_j^i(\xi; X)$ and $S_{jk}^i(\xi; X)$ are the Green’s function and the stress tensor on the monitoring surface due to a unit impulsive force at X in direction i , T_j^M is the traction on the monitoring surface due to the seismic source, u is the displacement on the monitoring surface, and n is the normal to the monitoring surface. The operator $*$ denotes convolution, and the summation convention is assumed.

In the cases we have done previously, 2D finite-difference and 3D finite-element calculations were performed to model the nuclear explosion, and the stresses and displacements from the calculation were saved on a surface in the elastic region outside the region of complex nonlinear behavior. We then invoked the representation theorem and integrated the stresses and displacements with an appropriate Green’s function to calculate the displacement at any point outside the calculation. We performed such calculations using Green’s functions for far-field body waves, for modes, and for full regional waveforms using wave number integration. The technique used for surface waves is

similar to the method of Bache et al. (1982). The Green's functions for the complete seismograms are derived from an algorithm based on the work of Luco and Apsel (1983) and Apsel and Luco (1983). The Green's functions for body waves are generated by a procedure similar to that described by Bache and Harkrider (1976) using a saddle point approximation to calculate a far-field plane wave for a given takeoff angle from a source in a plane-layered medium. Although the full waveform Green's functions generate the complete waveform, the other Green's functions can provide additional insight into the source and waveform generation.

Development of 3D Models for Calculations

The previous sections show that we can calculate explosions in 3D heterogeneous media and propagate the results of those calculations. The remaining question is whether the calculations are meaningful. That is, is the heterogeneity in the model consistent with the actual heterogeneity in the earth, and is the calculated wave motion consistent with the observed wave motion? We know that we can perform axisymmetric calculations that reproduce many of the characteristics of explosion-generated waveforms, and we have good material models that have been validated over many years. So we need to determine what 3D heterogeneous characteristics are important. There are two obvious common types of heterogeneity: (1) variability in elastic properties (moduli and density) and (2) variability in strength. Measurement of granite properties near SHOAL, for example, show density ranging from 2.4 to 2.7 gm/cm³, compressional velocity ranging from 5.27 to 5.7 km/s, and shear velocity ranging from 2.89 to 3.11 km/s. This is enough difference to cause distortion in the wavefront as it passes through the granite media.

Variability in strength is likely to be the stronger effect. Almost all rock is cracked and jointed, and although the cracks and joints are under substantial overburden pressure, they are still much weaker than the intact rock, and the rock as a whole will be weaker if it contains a higher density of cracks and joints. In our previous work on modeling near-field data in Degelen granite (Stevens et al, 2003), we found that rock strength could be modeled fairly well by several nonlinear models but that the strength varied substantially, with the rock near a few explosions exhibiting much higher strength than rock near other explosions. So our initial efforts to model nonlinear variability will be to use a variable-strength model based on a distribution of cracks and joints in the rock, with crack size and density based on nuclear test site observations and measurements.

Using data from site reports of underground nuclear tests in the United States, the former Soviet Union, and other sites as available, we plan to develop 3D models with a level of heterogeneous complexity consistent with these data. We will use site reports for U. S. nuclear tests to assess the heterogeneity in subsurface rock, using measurements of moduli and density and strength, where available, together with information about cracks and joints that weaken the rock matrix. In addition, through our previous joint projects with the Institute for the Dynamics of the Geospheres in Moscow, Russia (Stevens et al, 2001, 2002, 2003; Rimer et al, 1998, 1999), we have measurements taken from rock at the former Soviet Degelen test site that we will use to develop models of subsurface media heterogeneity in that environment. The measurements include moduli and density and both pre- and post-shot fracture density. Figure 5, for example, shows the pre-shot fracture density measured in drift walls prior to three Degelen explosions (details are given in Rimer et al, 1998). The amount of variability in fracture density implies a corresponding variability in rock strength.

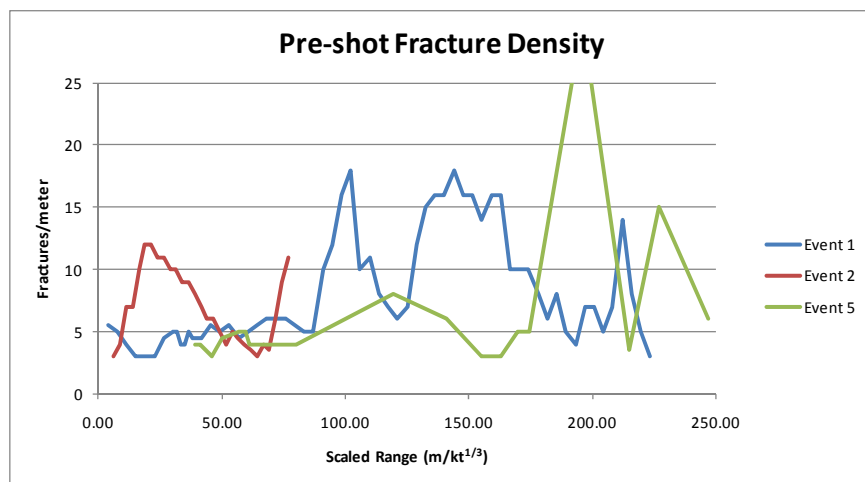


Figure 5. Pre-shot fracture density measurements prior to three Degelen explosions (from Rimer et al., 1998).

NPE Calculation

As our first calculation of a historical event with 3D heterogeneity, we model the NPE, including the surface topography. We have previously modeled this event in a 2D axisymmetric calculation (Stevens et al, 2004) and used the same material properties, which were derived from Rimer et al (1994) for the 3D calculation. The NPE was a chemical explosion with yield equivalent to 1 kt of TNT. The material geology at the NPE site is based on that of the nearby Misty Echo event and consists of four layers. Layers 1 and 4 are nonporous; layers 2 and 3 have porosities of 3% and 0.5%, respectively. The explosive is 1.315 kt of a 50/50 ANFO/emulsion mix in a cylindrical cavity centered at 389 m depth and measuring 7.7 m in radius (horizontally) and 5.2 m in height (vertically). The region of nonlinear deformation near the explosion is approximately spherical, but elongated and slightly offset vertically. The region of cracking is confined to near the free surface. This explosion is deeply overburied, so there is less asymmetry than in a normally buried explosion.

We calculated full waveform synthetics from this calculation at a distance of 400 km using the representation theorem with a full waveform Green's function. Figure 6 shows the region of yielding and cracking, conditions that generate shear waves, from the simulated NPE explosion (left). On the right, we compare data recorded at 400 km (top) and synthetics from a point explosion, a compensated linear vector dipole (CLVD) source, and from the source shown on the left. Because this is a very low velocity structure, the crust effectively traps P->S converted waves from the explosion, so the full waveform, including the Lg phase from the complex explosion source, is modeled quite well by a point explosion source.

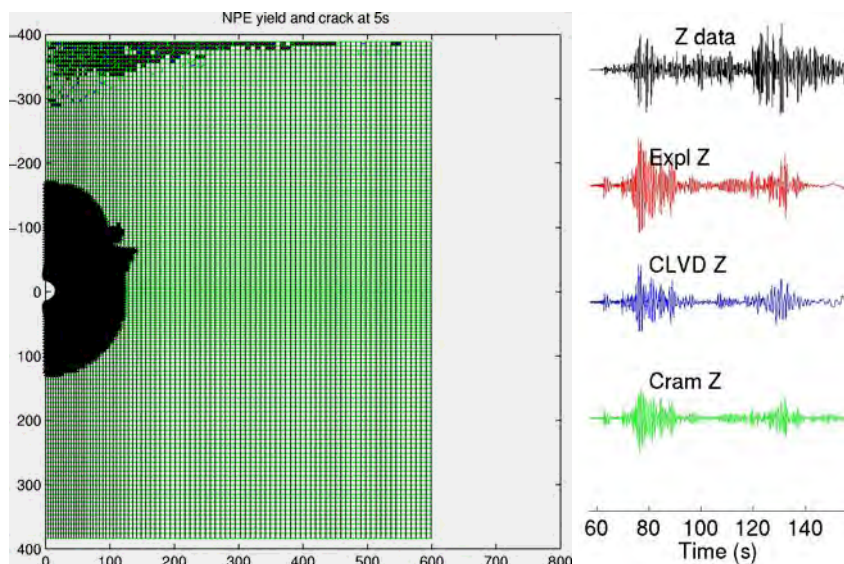


Figure 6. Region of nonlinear deformation and cracking from the NPE calculation (left). The near-circular area of deformation is similar to that of a point explosion. On the right is a vertical seismogram at 400 km from the NPE (top) and corresponding synthetics for a point explosion, a CLVD, and the nonlinear source model at the same depth. (1 kt at 390-m depth).

Figure 7 shows the actual topography near the NPE (Myers et al, 2007). For this first calculation, we modeled the area within 650 m of the explosion. Even that relatively small area has substantial topography, with elevation differences of up to 140 m. The strongest topographic changes are along a canyon to the north and a ridge to the south.

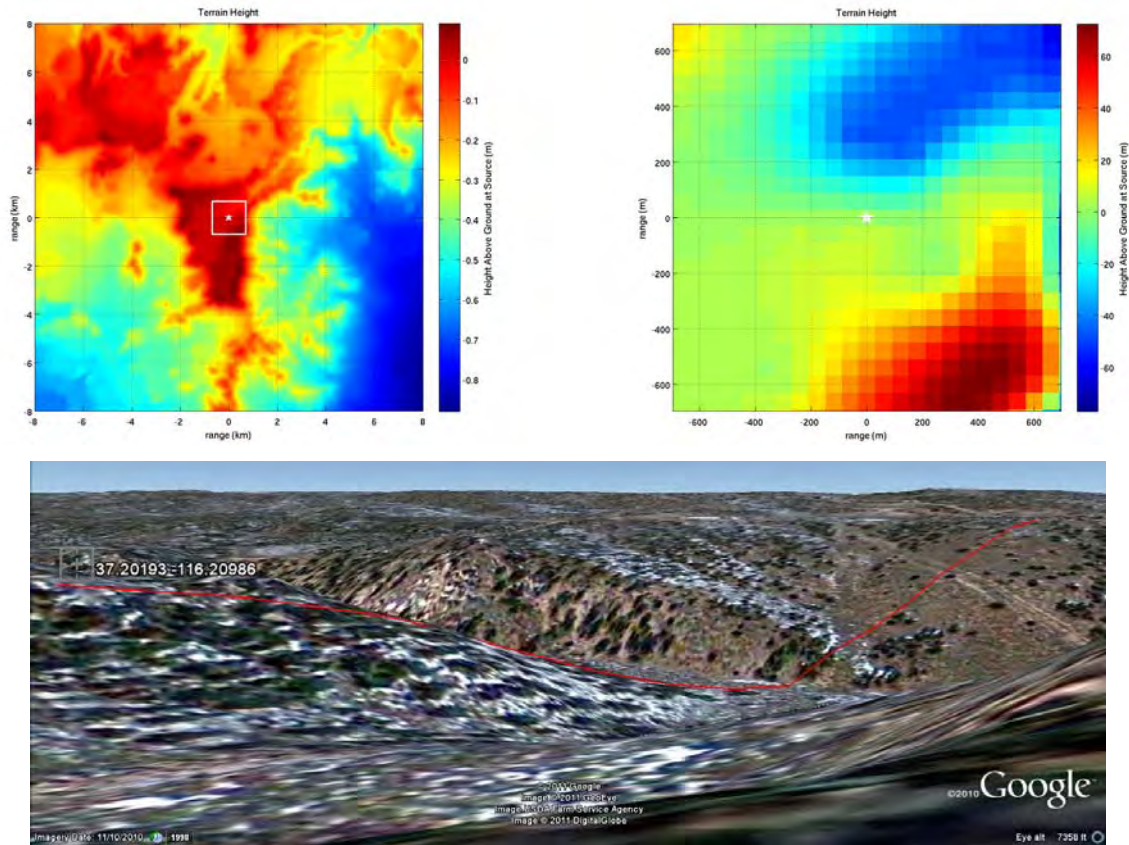


Figure 7. Topography within 8 km of the NPE (top left) and the location (top left, white square) and topography on the CRAM grid surface (top right). Lower figure shows a line due north from directly above the explosion to the edge of the grid.

Figure 8 shows nonlinear deformation and cracking at two times, showing the creation of the nonlinear near-source zone and surface spall and cracking. Except for the surface shape and associated cracking, the results are very similar to the axisymmetric results shown earlier. Surface spall and cracking are cut off 420 m from the origin.

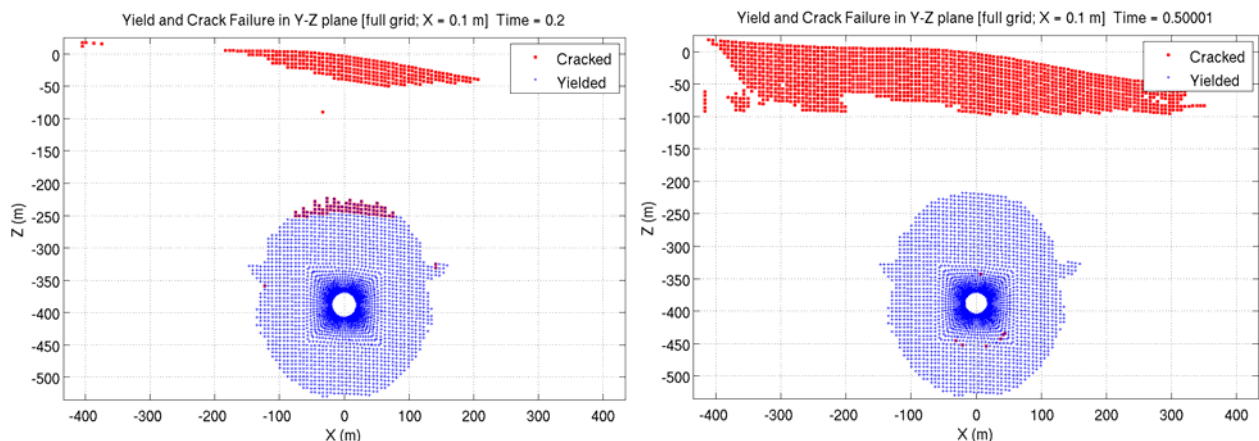


Figure 8. Nonlinear deformation (blue) and cracking (red) at 0.2 and 0.5 seconds from left to right along a north-south cross section through the source.

For comparison purposes, we also ran a calculation without topography, which gave results very similar to the axisymmetric calculation. We then used the representation theorem to calculate waveforms from both calculations at

a distance of 10 km to the north, in the direction indicated by the red line on Figure 7. The upper part of the Earth model used is listed in Table 1. This model is a merged version of the local NPE model of Rimer et al (1994), and the regional 3D model of Myers et al (2007). The Q structure used in the calculation is based on Swanger’s Law, $Q = \beta/10$, where β is shear velocity.

Table 1. Earth model used for NPE wave propagation

Depth (m)	P Velocity (m/s)	S Velocity (m/s)	Density (kg/m ³)
102	3586	1809	2200
328	1824	1000	1663
704	2701	1357	1900
3600	3210	1900	1680
3660	4500	2600	2300
8100	5930	3500	2430

The waveforms at 10 km are shown in Figure 9. Waveforms are generally similar, and the differences between the calculations with and without topography for the radial and vertical components are small. However, there is a substantial transverse component generated for the case with topography that is absent with the flat surface. The transverse component, which appears to be a Love wave, is about ¼ the maximum amplitude of the vertical component.

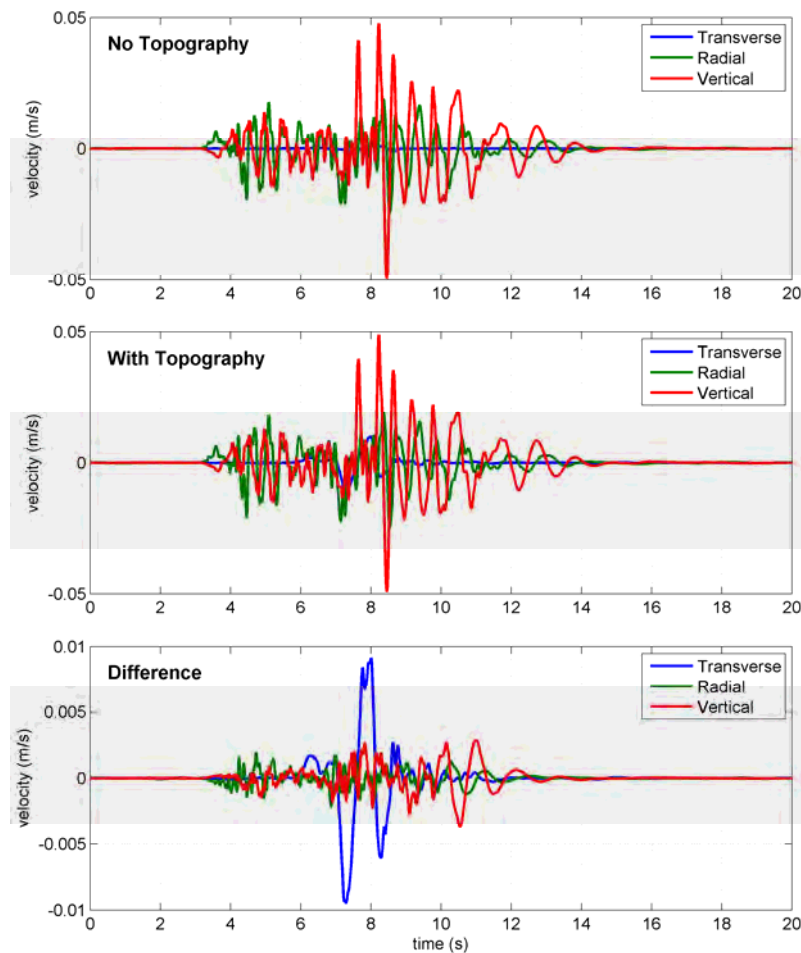


Figure 9. Three component waveforms at a distance of 10 km without (top) and with (middle) topography, and the differences between the waveforms (bottom).

CONCLUSIONS AND RECOMMENDATIONS

We are in the early stages of a new project to understand the effects of 3D structural variations on seismic waves from underground explosions. One of the main objectives is to understand why shear waves generated by underground explosions are ubiquitous. To that end, we will be using a 3D nonlinear finite-element program developed during a previous project to run calculations with 3D heterogeneity, based on the actual subsurface variability at test sites. We have run a calculation of the NPE with and without topography, for distances out to 650 m from the sources, extended to 10 km with the representation theorem. The calculation shows generation of an SH wave, apparently a Love wave, not present in the calculation without topography. We will be continuing the calculation, extending it to larger distances to include more topography, as well as running calculations to answer the more-general question about S generation from underground explosions.

ACKNOWLEDGEMENTS

We thank Steve Myers of Lawrence Livermore National Laboratory for providing the 3D earth model and topography for the NPE site.

REFERENCES

- Apsel, R. J. and J. E. Luco (1983). "On the Green's functions for a layered half-space. Part II," *Bull. Seismol. Soc. Am.* **73**: 931–951.
- Bache, T. C. and D. G. Harkrider (1976). "The body waves due to a general seismic source in a layered Earth model," *Bull. Seismol. Soc. Am.* **66**: 1805–1819.
- Bache, T. C., S. M. Day, and H. J. Swanger (1982). "Rayleigh wave synthetic seismograms from multi-dimensional simulations of underground explosions," *Bull. Seismol. Soc. Am.* **72**: 15–28.
- Luco, J. E. and R. J. Apsel (1983). "On the Green's functions for a layered half-space. Part I," *Bull. Seismol. Soc. Am.* **73**: 909–929.
- Myers, Stephen C., Jeffery L. Wagoner, and Shawn C. Larsen (2007). "Numerical experiments investigating the source of explosion S-waves," in *Proceedings of the 29th Monitoring Research Review: Ground-Based Nuclear Explosion Monitoring Technologies*, LA-UR-07-5613, Vol. I, pp.175–184.
- Rimer, N., W. Proffer, E. Halda, and R. Nilson (1994). "Containment related phenomenology from Chemical Kiloton," Maxwell Laboratories technical report to Defense Nuclear Agency, SSS-DTR-94-14405.
- Rimer, N., K. Lie, J. L. Stevens, J. R. Murphy, and G. G. Kocharyan (1998). "A micro-mechanical damage model for estimating seismic source characteristics of underground explosions in hardrock," Maxwell Technologies technical report to Defense Special Weapons Agency, MFD-DTR-98-15985, January.
- Rimer, N., J. L. Stevens, J. R. Murphy, and G. G. Kocharyan (1999). "Estimating seismic source characteristics of explosions in hardrock using a micro-mechanical damage model," Maxwell Technologies final report MTSD-DTR-99-16423, July.
- Stevens, J. L., N. Rimer, H. Xu, G. E. Baker, and S. M. Day (2003). "Near field and regional modeling of explosions at the Degelen test site," SAIC final report to the Defense Threat Reduction Agency, SAIC-02/2050, January.
- Stevens, J. L., N. Rimer, H. Xu, G. E. Baker, G. G. Kocharyan, B. Ivanov, and S. M. Day (2002). "Near field and regional modeling of explosions at the Degelen test site," SAIC Annual Report No. 2, submitted to, SAIC-02/2019, June.
- Stevens, J. L., N. Rimer, H. Xu, G. G. Kocharyan, B. Ivanov, and S. M. Day (2001). "Near field and regional modeling of explosions at the Degelen test site," SAIC Annual Report No. 1, submitted to the Defense Threat Reduction Agency, SAIC-01/1039, June.

2011 Monitoring Research Review: Ground-Based Nuclear Explosion Monitoring Technologies

- Stevens, J. L., G. E. Baker, H. Xu, T. J. Bennett, N. Rimer, and S. M. Day (2004). "The physical basis of Lg generation by explosion sources," SAIC final report submitted to the National Nuclear Security Administration under contract DE-FC03-02SF22676, December.
- Stevens, J. L. and G. E. Baker (2009). "Seismic wave generation by a non-isotropic explosion source," *J. Geophys. Res.* **114**: B12302, doi:10.1029/2008JB005965.
- Stevens, Jeffrey L. and Heming Xu (2010). "Wave propagation from complex 3D sources using the representation theorem," in *Proceedings of the 2010 Monitoring Research Review: Ground-Based Nuclear Explosion Monitoring Technologies*, LA-UR-10-05578, Vol. I, pp. 519–528.
- Stevens, Jeffrey L., Heming Xu, Michael O'Brien, Walter Nagy, and Norton Rimer (2011). "Wave propagation from complex 3D sources using the representation theorem," SAIC final report SAIC-11/3003 to the Air Force Research Laboratory, AFRL-RV-HA-TR-2011-1019, March.